EIGHTEENTH EUROPEAN ROTORCRAFT FORUM

BU - 08

Paper Nº 77

# A TRANSLATIONAL RATE COMMAND CONTROL LAW FOR HOVER ASSIST

R. SUIKAT
INSTITUTE FOR FLIGHT GUIDANCE
DLR (GERMAN AEROSPACE RESEARCH ESTABLISHMENT), GERMANY

September 15-18, 1992
AVIGNON, FRANCE

ASSOCIATION AERONAUTIQUE ET ASTRONAUTIQUE DE FRANCE

# A TRANSLATIONAL RATE COMMAND CONTROL LAW FOR HOVER ASSIST

Reiner Suikat
Institute for Flight Guidance
DLR (German Aerospace Research Establishment)
Braunschweig, Germany

ABSTRACT

Future helicopters will rely heavily on advanced flight control systems to extend bad weather operations and to fully utilize the operational envelope of the vehicle. Especially in hover the pilot workload can be significantly reduced by providing advanced command and stability augmentation functions. This paper documents the design and flight testing of a translational rate command (TRC) control law including position/altitude/heading hold functions which completely stabilizes the helicopter and decouples the inputs. Without pilot inputs the control law switches into hold modes, so that precision hover is done automatically. The control law has been validated in nonlinear simulations as well as flight tests on the BO105-S3 fly-by-wire/fly-by-light research helicopter of DLR. Discrete-time multivariable control design techniques have been used to derive the new control law demonstrating the applicability of such techniques to complex nonlinear systems.

## 1. INTRODUCTION

Due to the demand for extended bad weather and single pilot operations advanced control systems are becoming increasingly important in modern helicopters. These systems can provide significant reductions in pilot workload owing to stabilization of the aircraft and decoupling of the control inputs. Especially in hover the reductions in pilot workload achieved with advanced stability and control augmentation systems are remarkable.

The basic dynamic behavior of a helicopter, whether stability augmentation is being used or not, can be classified into certain response types, which describe the way in which the helicopter responds to a pilot input. The inherent response type of most helicopters is a rate command response, i.e. the rotational rates correspond to the pilot inputs. The benefits of various response types have been studied by Hoh[1], who concludes that in most situations pilots prefer a rate command response type. However, in poor visibility and hover better pilot ratings are achieved with attitude command and for certain high gain maneuvers such as sidestep and dash a translational rate command (TRC) response yields the best pilot ratings. Translational rate command implies that the translational velocity of the helicopter is directly controlled by stick inputs.

This paper documents the design and flight testing of a TRC control law including position/altitude/heading hold functions. Any pilot input is translated into a commanded value of the corresponding motion variable, which are forward and transverse velocity for cyclic stick input, climb rate for collective input, and turn rate for pedal input. Whenever the pilot input is smaller than a certain threshold the hold function in the corresponding channel is engaged automatically, thus precision hover above a given spot is achieved without any pilot activity.

Previous examples of control laws providing velocity vector control in hover can be found in the ADOCS (Advanced Digital/Optical Control System) program of Boeing Vertol[2] and the McDonnell Douglas Helicopter AV-05 Flight experiment program[3]. Both programs demonstrate a significant reduction in pilot workload. The AV-05 flight control system however is not a translational rate command system, since the command variable is the aircraft acceleration. The velocity vector is maintained in the North/East reference frame so that the inertial velocity vector is held independent of yaw. The control law described in this paper maintains the velocity vector in the aircraft reference frame, so that a heading change will result in a coordinated turn. Both the ADOCS and the AV-05 control laws are based on classical control design methods, whereas the control law presented here is based entirely on discrete-time multivariable control design methods demonstrating the applicability of modern control theory to complex real world systems.

## 2. CONTROL LAW STRUCTURE

In this section the equations for the TRC control law are derived. The control law uses discrete-time multivariable control design methods with separate feedback and feedforward paths. The feedback path is based on a proportional+integrator+filter (PIF) regulator algorithm which is implemented in incremental form. To compute the feedback gains an eigenstructure assignment method is used and, to accommodate the significant nonlinearities of the helicopter, an optimal gain scheduling method is applied. The feedforward path is based on a non-zero setpoint formulation, however, an explicit model following algorithm is currently being implemented to enhance the performance of the system.

### PIF Controller

As mentioned before the feedback control is based on a proportional+integral+filter[4] structure. Consider the linear system given by the discrete-time state equation

(1) $$x_{k+1} = \Phi x_k + \Gamma u_k .$$

This system equation is then augmented with a filter equation. Here the control deflections are expressed as an Euler integration of the control rates,

(2) $$u_{k+1} = u_k + T v_k ,$$

where $T$ is the sample time. Finally, integrator states are also added,

(3) $$\xi_{k+1} = \xi_k + T y_k$$

where the integrator states $\xi$ are an Euler integration of the system outputs $y$. The addition of these extra system states provides several benefits. The filter states limit the bandwidth of the controller output and thereby the susceptibility of the controller to high frequency noise, at the same time they also prevent large step commands to the actuators, while the integrator states provide perfect steady state tracking of the output variables. These equations are now combined to form the PIF system equation:

(4) $$\begin{bmatrix} x \\ u \\ \xi \end{bmatrix}_{k+1} = \begin{bmatrix} \Phi & \Gamma & 0 \\ 0 & I & 0 \\ TC & TD & I \end{bmatrix} \begin{bmatrix} x \\ u \\ \xi \end{bmatrix}_k + \begin{bmatrix} 0 \\ TI \\ 0 \end{bmatrix} v_k$$

A linear constant gain feedback control is applied:

(5) $$v_k = -K_x x_k - K_u u_k - K_\xi \xi_k$$

The feedback gain matrices $K_{x,u,\zeta}$ may be computed using any method for linear discrete-time controller design. In the current research a standard eigenstructure method[5] is used, since this provides an easy way of satisfying the bandwidth requirements in the handling qualities specifications and also to shape the modes of the system, which is needed for dynamic decoupling.

Gain Scheduling

A significant problem in the computation of the feedback gains is posed by the nonlinearities of the helicopter. The most important nonlinear terms are the kinematic coupling terms, e.g. in the longitudinal equation of motion[6]:

(6) $$m(\dot{U} - VR + WQ) = mg_x + F_x$$

the terms $VR$ and $WQ$. Early simulation results indicated that these nonlinearities demand a gain scheduled control law. Presently the feedback gains are scheduled with respect to the three kinematic velocity components $u$, $v$, and $w$ using a special scheduling algorithm that computes gain matrices which minimize the errors in the eigenstructure assignment over all design points[7]. This optimal gain scheduling algorithm is described in the following paragraphs.

A quadratic gain schedule in one variable, in this case $u$, is given by

(7) $$K = K_0 + K_1 u + K_2 u^2.$$

The simplest way to compute the coefficient matrices $K_{0,1,2}$ is to compute individual gain matrices at a number of design points and use a least squares approximation to obtain the coefficient matrices. Unfortunately a least squares approximation cannot account for the performance of the scheduled gains. To this end an optimal pole-placement gain-scheduling algorithm has been devised that minimizes the errors in the eigenstructure assignment over all design points. This algorithm works by first recasting the scheduling problem into a constant-gain output-feedback problem[8]. Consider a constant output-feedback control $u = -KCy$, then a quadratic schedule according to Eq. (7) is achieved by setting

(8) $$K = [K_0 \;\; K_1 \;\; K_2]$$

and

(9) $$C = \begin{bmatrix} C \\ uC \\ u^2 C \end{bmatrix}.$$

The constant-gain output-feedback problem is solved following the procedure given in Ref. 7 by minimizing the cost function:

(10) $$J = \sum_j \operatorname{tr}\left\{(KC_j - K_j)V_j Q_j V_j^T (KC_j - K_j)^T\right\}$$

where $Q_j$ is a diagonal weighting matrix,
$K_j$, $V_j$ are the gain matrices and closed-loop eigenvector matrices at the design points,
$K = [K_0 \; K_1 \; K_2]$ are the coefficient matrices to be computed, and
$C_j$ are the output matrices in the form given by Eq. (9) with $u = u_j$ being the velocity at the design point $j$.

The solution found by setting the partial derivative $\partial J/\partial K = 0$ is given as

(11)
$$K = \left(\sum_j K_j W_j C_j^T\right)\left(\sum_j C_j W_j C_j^T\right)^{-1},$$

where $W_j = V_j Q_j V_j^T$. This gain matrix $K$ yields a gain schedule with one parameter. To obtain the desired gain schedule with three parameters the following procedure is used: First separate gain schedules $K_U$, $K_V$, and $K_W$ are computed for $U$, $V$, and $W$. Then these gain schedules are combined into one schedule

(12)
$$K = \frac{1}{3}(K_{U0} + K_{V0} + K_{W0}) + \frac{U}{V_{tot}}\left(UK_{U1} + U^2 K_{U2}\right) + \cdots .$$

Here the contribution of each velocity component is scaled by the ratio of the velocity component and the total velocity.

## Feedforward Path

The feedforward path is responsible for good response to pilot inputs. Here a nonzero setpoint formulation is used, which means that the steady state output vector $y$ of the system will track a constant command vector $y_c$. The corresponding ideal values for the state and control vectors are then obtained as

(13)
$$x^* = S_x y_c$$
$$u^* = S_u y_c ,$$

where

(14)
$$\begin{bmatrix} \cdots & | & S_x \\ \cdots & | & S_u \end{bmatrix} = \begin{bmatrix} \Phi - I & \Gamma \\ C & D \end{bmatrix}^{-1}$$

is the inverse of the quad partition matrix of the linear system. While this definition is only valid for a constant command vector, experience has shown that good tracking is also achieved for slowly varying commands. In this case $x^*$ and $u^*$ are forming the so called 'star-trajectory'. It is also necessary to define star values for the integrator states $\xi$. These values define the change in the integrator states due to a command change. A linear relationship between the commanded output vector and the star values of the integrator vector

(15)
$$\xi^* = S_\xi y_c$$

is assumed. In the current research $S_\xi$ is set to be a diagonal matrix with negative entries, i.e. a command input in any variable will only affect the corresponding integrator state. The rationale for selecting a negative value is explained with a simple example in Fig. 1. In this figure the response of a simple linear system with constant gain feedback on the system states as well as an additional integrator state to a step input for several values of $S_\xi$ is shown. Since the system lags behind the step input, the integral of the output error, which is the area between the output curve and the step command, will initially become negative. If the controller is asked to drive this integral back to zero, i.e. if $S_\xi = 0$, then this can only be achieved with some overshoot. Selecting a negative value for $S_\xi$ on the other hand yields a response with little or no overshoot, depending on the particular value. Obviously the magnitude of $S_\xi$ should not be taken too large, since this will slow down the system response significantly. Indeed one can achieve a response characteristic such that the output will initially move into the wrong direction. Currently no algorithm is known to the author to compute the optimal values for $S_\xi$ and so the values are optimized using simulation runs.

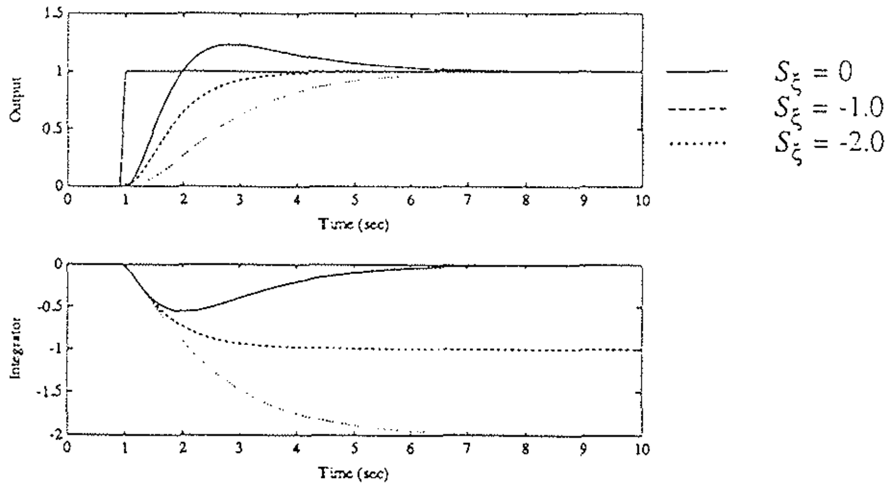


Fig. 1 Response of a simple system with integrator

The feedback control law is now modified such that the feedback gains multiply the differences between the actual and the star-values of the states, the controls, and the integrators:

(16) $$v_k = -K_x(x_k - x_k^*) - K_u(u_k - u_k^*) - K_\xi(\xi_k - \xi_k^*)$$

Incremental Control Law

The final step in the derivation of the control law equations is the incremental implementation, which provides the benefits of implicitly including a full sample period computation time (in conjunction with using filter states) and also allowing the use of the measured quantities rather than perturbation quantities in the control law. This second benefit is very important, since the control law in this form does not require any kind of trim tables or equations, but still provides automatic trim functions. The basic idea is to write down the difference between two successive sample steps:

(17)
$$v_{k-1} - v_{k-2} = -K_x\left(\left(x_{k-1} - x_{k-2}\right) - \left(x^*_{k-1} - x^*_{k-2}\right)\right) - K_u\left(\left(u_{k-1} - u_{k-2}\right) - \left(u^*_{k-1} - u^*_{k-2}\right)\right) - K_\xi\left(\left(\xi_{k-1} - \xi_{k-2}\right) - \left(\xi^*_{k-1} - \xi^*_{k-2}\right)\right)$$

It can be shown[4] that under the assumption of a constant command Eq. (17) is also valid for total values $X = X_0 + x$, i.e. the nominal values cancel out of the equation. Using

(18)
$$\xi_{k-1} - \xi_{k-2} = Ty_{k-2}$$

(19)
$$u_{k-1} - u_{k-2} = Tv_{k-2}$$

and

(20)
$$y_{c,k-1} = u_{c,k}$$

Eq. (17) can now be rewritten as

(21)
$$V_{k-1} = -K_x\left(X_{k-1} - X_{k-2}\right) + \left(I - TK_u\right)V_{k-2} - TK_\xi\left(Y_{k-2} - Y_{c,k-2}\right) + \left(K_x S_x + K_u S_u + K_\xi S_\xi\right)\left(U_{c,k} - U_{c,k-1}\right) .$$

Also

(22)
$$U_k = U_{k-1} + TV_{k-1} .$$

These are the equations that are actually implemented in the flight computer. Observe the following facts: The control position at time $k$ depends only on values of the state vector at or before time $k$-1, while the feedforward term achieves an immediate control response since $v_{k-1}$ depends on $u_{c,k}$. Note also that the computation of the star trajectory values is included implicitly in the feedforward term. The structure of this control law is depicted in Fig. 2.

## 3. TRC CONTROL LAW FOR HELICOPTER

The controller structure derived in the previous section is now applied to a helicopter control law providing translational rate command and position hold functions. Here the helicopter is described by an eight degrees of freedom linear model with the state vector $x = [u\ w\ q\ \theta\ v\ p\ r\ \phi]'$ and the control vector $u = [\delta_{col}\ \delta_{pitch}\ \delta_{roll}\ \delta_{ped}]'$. Since the control law shall provide tracking for translational velocity commands the output vector is selected to be $y = [U_g\ V_g\ \dot{H}\ \Psi]'$. While the implemented control law uses the nonlinear equations to compute the output variables from the measured state variables, this is not possible in the feedback gain design. Here the output vector is approximated by $y = [u\ v\ -w\ r]'$. Note that the body-axis coordinate system is defined such that the z-axis is pointing downward, hence $\dot{H}$ is approximated by $-w$.

The eigenvalues for the rotational modes as given in Table 1 have been selected to satisfy the bandwidth specifications given in the handling-qualities requirements[9]. Note that a large damping ratio is

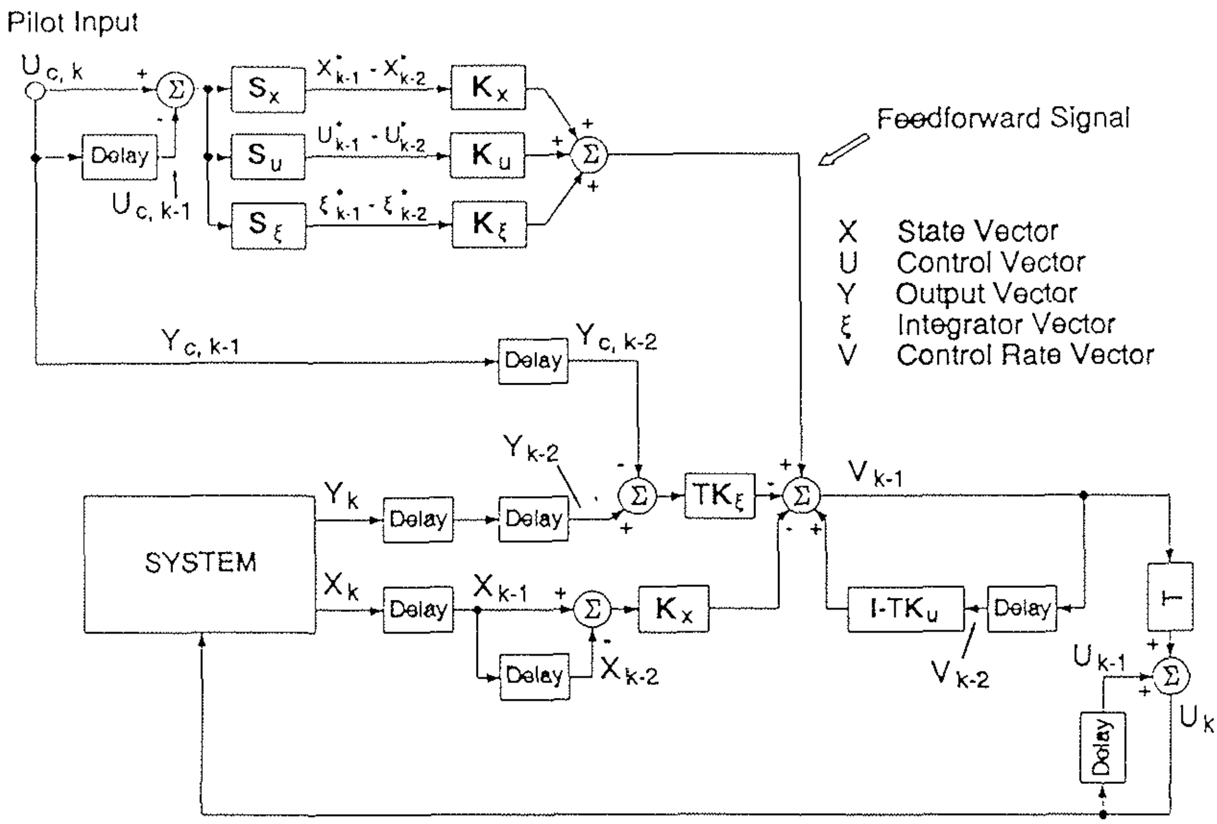


Fig. 2 Control law block diagram

Table 1 Design eigenvalues for TRC control law

| Mode | ω (rad/s) | ζ |
|---|---|---|
| 1) Pitch | 4.5 | 0.9 |
| 2) Roll | 5.0 | 0.9 |
| 3) Longitudinal motion | 0.2 | 1.0 |
| 4) Vertical " | 0.5 | 1.0 |
| 5) Lateral " | 0.3 | 1.0 |
| 6) Yaw | 6.0 | 1.0 |
| 7) Collective filter | 8.0 | 1.0 |
| 8) Cyclic pitch " | 14.0 | 1.0 |
| 9) Cyclic roll " | 15.0 | 1.0 |
| 10) Pedal " | 20.0 | 1.0 |
| 11) Long. vel. integrator | 1.0 | 1.0 |
| 12) Lat. vel. " | 1.2 | 1.0 |
| 13) Altitude rate " | 2.0 | 1.0 |
| 14) Yaw rate " | 1.5 | 1.0 |

selected for the two oscillatory modes to reduce oscillations. Past experience[7] has shown that the filter frequencies should be significantly higher than that of any aircraft mode. However, a fairly small bandwidth was selected for the collective filter, since any input to the collective actuator results in a change in required engine torque. The small bandwidth in this control channel reduces the required rate of the torque changes. The integrator eigenvalues are a compromise between small values (little coupling, but slow response to disturbances) and large values (fast response, but increased coupling).

To achieve the desired dynamic decoupling of the aircraft modes eigenvector shaping is applied. The design closed-loop eigenvectors are listed in Table 2. For example, the pitch mode eigenvector is such that the dominant element corresponds to $Q$, while the elements corresponding to $P$ and $R$ are both set to zero, resulting in a pure pitching motion for that mode. The filter and integrator eigenvectors are all designed such that the filters (or integrators) are fully decoupled.

Table 2 Design eigenvectors for TRC control law

| 1 | 2 | 3 | 4 | 5 | 6 | 7 | 8 | 9 | 10 | 11 | 12 | 13 | 14 | |
|---|---|---|---|---|---|---|---|---|---|---|---|---|---|---|
| x | x | 1 | x | x | x | x | x | x | x | x | x | x | x | $U$ |
| x | 0 | x | 1 | x | x | x | x | x | x | x | x | x | x | $W$ |
| 1 | 0 | x | x | 0 | 0 | x | x | x | x | x | x | x | x | $Q$ |
| x | x | x | x | x | x | x | x | x | x | x | x | x | x | $\Theta$ |
| x | x | x | x | 1 | x | x | x | x | x | x | x | x | x | $V$ |
| 0 | 1 | 0 | 0 | x | x | x | x | x | x | x | x | x | x | $P$ |
| 0 | x | 0 | 0 | x | 1 | x | x | x | x | x | x | x | x | $R$ |
| x | x | x | x | x | x | x | x | x | x | x | x | x | x | $\Phi$ |
| x | x | x | x | x | x | 1 | 0 | 0 | 0 | x | x | x | x | Coll. |
| x | x | x | x | x | x | 0 | 1 | 0 | 0 | x | x | x | x | Pitch |
| x | x | x | x | x | x | 0 | 0 | 1 | 0 | x | x | x | x | Roll |
| x | x | x | x | x | x | 0 | 0 | 0 | 1 | x | x | x | x | Pedal |
| x | x | x | x | x | x | x | x | x | x | 1 | 0 | 0 | 0 | $U_g$ |
| x | x | x | x | x | x | x | x | x | x | 0 | 1 | 0 | 0 | $V_g$ |
| x | x | x | x | x | x | x | x | x | x | 0 | 0 | 1 | 0 | $H_g$ |
| x | x | x | x | x | x | x | x | x | x | 0 | 0 | 0 | 1 | $\Psi$ |

where: '0' element shall be exactly zero
'1' element shall be the largest
'x' element may have any value

## Hold Functions

In addition to the control law described so far position/altitude/heading hold functions are implemented as separate outer loops. For each channel constant gains are applied to the position error as well as the rate to obtain artificial pilot commands for the TRC control law. Since the output vector used in the TRC control is defined to be translational velocity, climb rate, and heading rate, it can be used directly for the rate feedback of the hold functions. The position error is computed as a simple integral of the translational velocities, while the altitude and heading errors are obtained from the sensor equipment. As an example the structure of the position hold function is shown in Fig. 3.

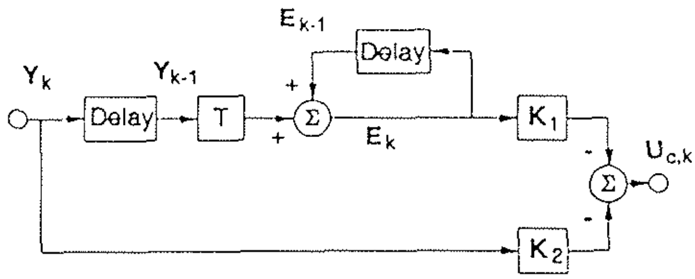


Fig. 3 Hold function implementation

The hold functions are activated automatically whenever no pilot inputs are applied to the system, they can also be switched off completely to better investigate the performance of the inner control loops.

## 4. CONTROL LAW VALIDATION

The control law described in the previous sections has been validated using nonlinear simulations and flight tests. The BO105-S3 research helicopter of DLR was flown with the TRC control engaged at forward speeds ranging from -20kts to +40kts, sideways ±20kts, climb rates of ±1000ft/min, and turn rates of ±90deg/sec. Wind speeds during the test flights were up to 30kts. All modes of the control law have been exercised during the flight tests and no major problems were encountered. There was a slight pitch-roll oscillation with a frequency of about 0.5Hz, which the pilots found somewhat annoying, as well as some residual coupling between the inputs. These problems are due to modeling errors and the use of a simple feedforward structure in the control law and will be resolved for the next flight test campaign.

### Flight Test Setup

In this paragraph the general setup for the flight tests is described. The BO105-S3 research helicopter is equipped with a simplex full authority fly-by-wire/fly-by-light system controlled by the test pilot using regular flight controls. A full mechanical backup is provided for the safety pilot who can take control of the aircraft at any time by simply overpowering the fly-by-wire actuators, which are coupled into the mechanical controls with springs, hence a redundant fly-by-wire control system is not needed. The sensor package consists of a strapdown attitude and heading reference system, digital air data computer, and Doppler radar. The pilot control panel allows mode selection and in flight parameter adjustments using software controlled switches and potentiometers.

The test engineer coordinates and monitors the flight tests from the ground. For this purpose a PCM data link between the helicopter and the ground station is provided that transmits flight data and also intercom voice connection. The ground station is equipped with a video display to observe the helicopter, a quicklook screen display, strip chart recorders, and data storage on analog tape as well as hard disk.

### Flight Test Results

In the following paragraphs some examples are shown to demonstrate the capability of the proposed control law.

Forward velocity command

Fig. 4 shows the response of the helicopter to a series of forward velocity command inputs. The pilot input is filtered with a first order lag filter to dampen the response of the controller, this filtered signal is shown in the figure (dashed line in upper left plot). Since the helicopter first needs to pitch in order to accelerate, the delay of the response (continuous line) is quite natural. While most of the activity in the pitch angle and control deflection curves is due to the command changes, the small oscillation which was mentioned earlier can also be observed. The sharp deceleration command at $t$=37 sec from about 20 kts to hover results in a rapid pitch-up from -10 deg to about 20 deg. This rapid pitching motion leads in turn to an undesired climb which can be attributed mainly to the simple feedforward structure used in the current control law design.

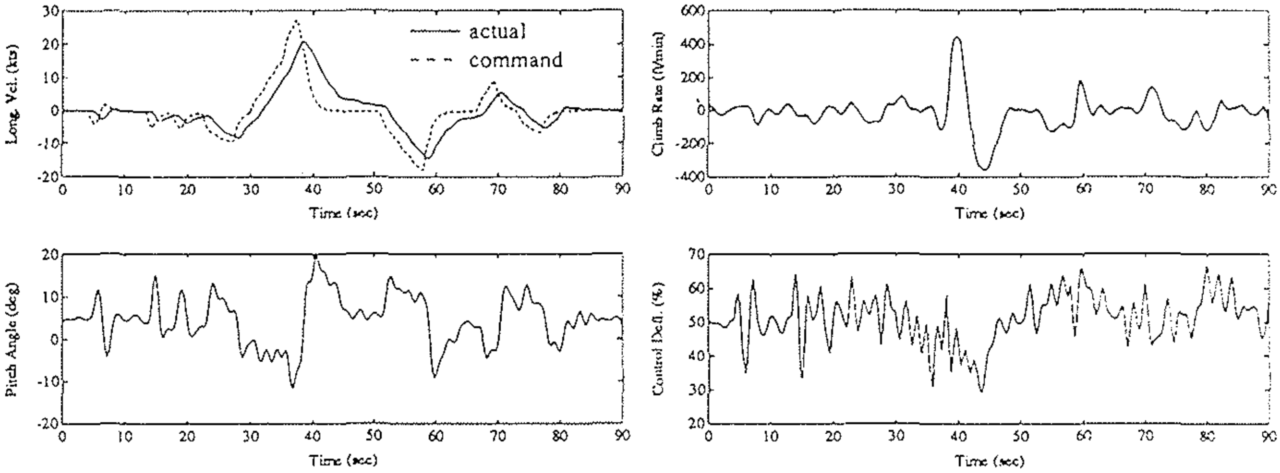


Fig. 4 Response to forward velocity commands (Ground speed and pitch angle)

Lateral velocity command

The response of the helicopter to a lateral velocity input is shown in Fig. 5. Again good tracking of the command is achieved. As in the previous example rapid changes of the commanded velocity result in an undesired climb rate, here the peak is at about 200ft/min (about 1m/s). In addition a significant heading change of almost 30 deg can be observed. This heading change can be attributed to errors in the aerodynamic model leading to an overcompensation of the open loop coupling, which is negative yaw due to positive $v$.

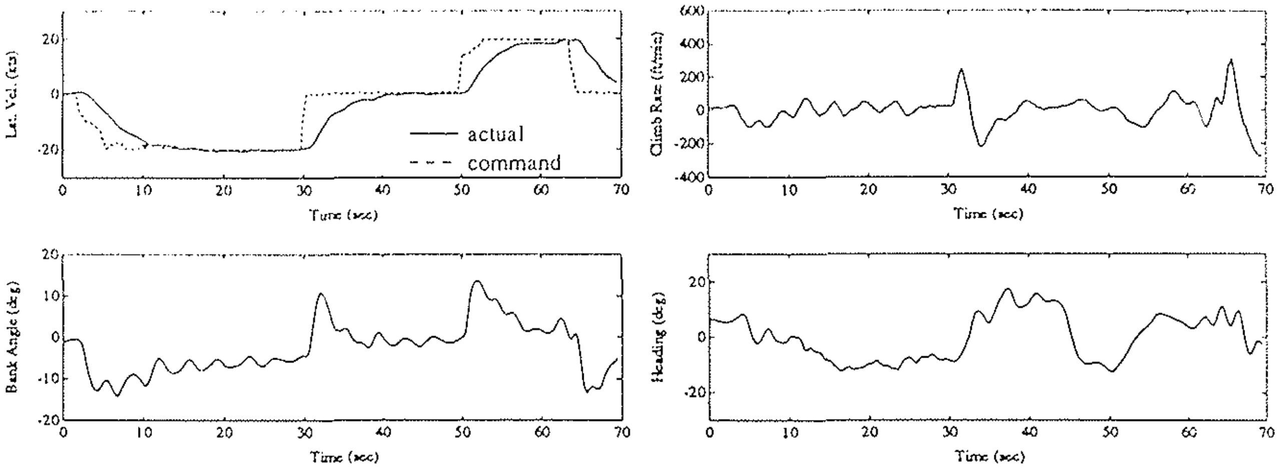


Fig. 5 Response to lateral velocity commands (Ground speed and bank angle)

Position hold

In Fig. 6 the accuracy of the position hold loop is demonstrated. At wind speeds ranging from 10-20kts the position error with respect to the internally generated position reference stays less than 0.5m. Since no sensor signal is available for position measurement, the position is computed from the Doppler radar signal and therefore offsets in the Doppler radar signal will cause a drift in position. This drift can neither be measured nor compensated for internally and depends entirely on the accuracy of the Doppler radar.

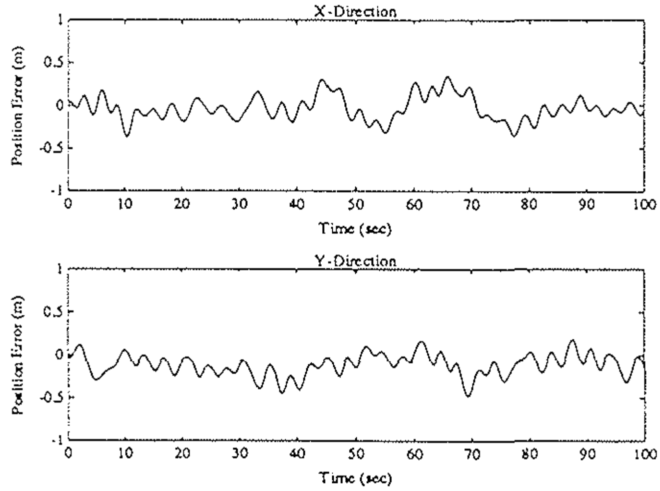


Fig. 6 Position error with position hold engaged, wind speed 10-20kts

## 5. CONCLUSIONS

A translational rate command control law has been developed and flight tested on a fly-by-wire helicopter by DLR showing significant reductions in pilot workload and thereby freeing up the pilot for other tasks. The control law provides velocity vector and heading control plus position/altitude/heading hold functions. In addition turn coordination is achieved automatically, i.e. a heading change will result in a coordinated turn. All modes of the control law have been validated during the flight tests. Tracking of velocity commands was found to be good, but some coupling was observed, the main problem being climb rates resulting from rapid pitching motions during acceleration or deceleration. This coupling can be attributed to the simple feedforward structure used in the initial flights. Currently an explicit model following algorithm is being implemented to eliminate this coupling. A slight pitch-roll oscillation with a frequency of about 0.5 Hz was also observed, this oscillation is a result of modeling errors and should also be eliminated for the next flight test campaign.

The control law was designed using discrete-time multivariable control design methods demonstrating the applicability of modern control design methods for linear systems to complex and highly non-linear systems. The computation of the required feedback and feedforward matrices is completely automated using MATLAB[10] programs. It should be pointed out that tuning individual loop gains is practically impossible with this type of control law design. Gain matrices are changed by modifying design parameters like desired pole locations and/or corrections to the linear models of the helicopter.

## 6. REFERENCES


1. R.H. Hoh, Dynamic requirements in the new handling qualities specifications for U.S. military rotorcraft, Proceedings of the International Helicopter Handling Qualities and Control Conference, Paper No. 4, 1988.

2. K.H. Landis and S.I. Glusman, Development of ADOCS controllers and control laws, NASA CR-177339, Volume 2, 1987.

3. B.P. Gupta, B.B. Barnes, G. Dockter, R. Hodge and C. Morse, Design development and flight evaluation of an advanced digital flight control system, AHS 43rd annual forum, May 1987.

4. J.R. Broussard, Design, implementation, and flight testing of PIF autopilots for general aviation aircraft, NASA CR-3709, 1983.

5. A.N. Andry, E.Y. Shapiro and C.J. Chung, On eigenstructure assignment for linear systems, IEEE Trans. on aerospace and electronic systems, AES-19, pp 711-729, 1983.

6. J. Roskam, Airplane flight dynamics and automatic flight controls, Roskam Aviation and Engineering Corp., Ottawa, Kansas, 1979.

7. R. Suikat, An optimal pole placement gain scheduling algorithm using output feedback, PhD. thesis, The University of Kansas, Department of aerospace engineering, 1990.

8. D.R. Downing and J.R. Broussard, Digital flight control - analysis and design, Short course notes, The University of Kansas, Division of continuing education, 1990.

9. Handling qualities requirements for military rotorcraft, Aeronautical design standard, US Army Aviation Systems Command, ADS-33C, 1989.

10. MATLAB (MATrix LABoratory), The MathWorks Inc., Natick, Ma.